Available online at www.sciencedirect.com
SCIENCE DIRECT®
Journal of Solid State Chemistry 178 (2005) 1139–1144
JOURNAL OF SOLID STATE CHEMISTRY
www.elsevier.com/locate/jssc

Synthesis and characterization of flowerlike ZnO nanostructures via an ethylenediamine-meditated solution route

Xiangdong Gao*, Xiaomin Li, Weidong Yu

State Key Laboratory of High Performance Ceramics and Superfine Microstructures, The Shanghai Institute of Ceramics, The Chinese Academy of Sciences, DingXi Road, Number 1295, Shanghai 200050, People's Republic of China

Received 10 August 2004; received in revised form 10 October 2004; accepted 13 October 2004

Abstract

Flowerlike ZnO nanostructures were deposited on Si substrate by choosing hexamethylenetetramine as the nucleation control reagent and ethylenediamine as the chelating and capping reagent. Structural and optical measurements reveal that obtained ZnO exhibits well-defined flowerlike morphology, hexagonal wurtzite structure, uniform distribution on substrate, and strong photoluminescence in ultraviolet band. The well-arrayed pedals of each ZnO flower possess the typical tapering feature, and are built up by many well-aligned ZnO nanorods. Moreover, each single nanorod building up the pedal exhibits the single crystal nature and the growth direction along *c*-axis. Effects of the precursor composition on the morphology of ZnO were discussed.

Keywords: ZnO; Flowerlike; Ethylenediamine; Nanostructure

1. Introduction

ZnO is one of the most important functional oxides with direct wide band gap (3.37 eV) and large excitation binding energy (60 meV), exhibiting many interesting properties including near-UV emission [1], transparent conductivity [2], and piezoelectricity [3]. The morphologically controllable synthesis of ZnO nanomaterials is spurred by the recent success on the realization of room-temperature ultraviolet lasing from nanorod array by Yang et al. [4,5]. Its great significance for the systematic fundamental study of structure–property relations and its wide variety of technological potentials as catalysts, selective separations, sensor arrays, wave guides, drug carriers, biomedical implants with macroporosity, and photonic crystals with tunable band gap, have inspired vast research interests [6–16].

Up to now, well-defined ZnO nanostructures with abundant shapes have been achieved through the vapor-based techniques, such as nanoneedles [6], nanocables and nanotubes [7], nanowalls [8], nanobridges and nanonails [9], nanohelixes, nanosprings, nanorings [10,11], hierarchical nanostructures [12], and mesoporous polyhedral cages and shells [13]. Via the chemical solution route, tube-, tower- and flower-like ZnO nanostructures (FZNs) [5,14,15], and oriented helical ZnO nanorod array [16] have also been realized very recently. However, despite great progresses in this field, the shape controllable synthesis of ZnO nanocrystals, especially the control over the complex structure, is still very difficult.

Herein, we report a novel solution route to synthesize well-defined FZNs on Si substrate at low temperature (95 °C) and in a short reaction time (60 min), by the thermolysis of ethylenediamine (en)–zinc complex with the assistance of hexamethylenetetramine (HMT). Both en and HMT are commonly adopted organic substances in the synthesis of ZnO-based materials including thin films [17,18], nanorod and nanowire [19,20]. However, to our best knowledge, there is no research effort on the ZnO nanostructures with complex morphology by the

*Corresponding author. Fax: +86 021 52413122.
E-mail address: xdgao@mail.sic.ac.cn (X. Gao).

0022-4596/$ - see front matter © 2004 Elsevier Inc. All rights reserved.
doi:10.1016/j.jssc.2004.10.020

joint use of en and HMT by far. Therefore, the proposed simple and novel method to prepare FZNs and the fundamental controlling principle of en and HMT on the structure and morphology of ZnO crystals are especially meaningful for the morphological synthesis of ZnO and other similar oxide nanocrystals.

2. Experimental

All the chemicals were analytic grade reagents without further purification. In a typical synthesis (sample 1), the aqueous precursor of zinc–en complex was prepared by mixing analytical chemicals of zinc sulfate, en and HMT with the molar ratio of 1:3:1 and zinc concentration of 0.001 mol/L. The precursor was filled into a laboratory pyrex glass bottle with polypropylene autoclavable screw caps with the filling ratio of 80%. Si (111) wafers were placed in the bottom of the bottle for the harvest of products. The prepared precursor was heated from room temperature and maintained at the constant temperature of 95 °C for an hour in a regular laboratory oven. Subsequently, the obtained white layer was thoroughly washed with pure water to eliminate the residual of salts and organic substance, and dried in air for subsequent measurements.

The structural and morphological characterization of as-deposited sample was examined by D/max 2550 V diffractometer (Rigaku Ltd., Japan, CuK_α radiation), scanning electron microscope (JSM-6700F), transmission electron microscopy (TEM) and electron diffraction (JEOL-2010). The photoluminescence spectra were measured by RF-5301PC fluorescence spectrophotometer (Shimadzu Ltd., Japan) at room temperature with the excitation wavelength of 340 nm. A Xe lamp with a filter was used as the excitation light source. For the TEM measurement, ZnO flowers were peeled from the substrate by a surgical knife and attached on the copper grid for further analysis. For other measurements, the as-deposited sample on substrate is applicable and no additional treatment was required.

3. Results and discussion

During the thermolysis of the precursor at the elevated temperature, the zinc–en complex decomposes and Zn^{2+} was released (Eq. (1)), and HMT and the released en molecules experience the hydrolysis process, resulting in the formation of OH^- (Eqs. (2) and (3)).

$$[Zn(NH_2\cdot(CH_2)_2\cdot NH_2)_3]^{2+} \rightarrow Zn^{2+} + 3NH_2\cdot(CH_2)_2\cdot NH_2, \quad (1)$$

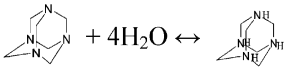

$$+ 4H_2O \leftrightarrow \quad + 4OH^- \quad (2)$$

$$NH_2\cdot(CH_2)_2\cdot NH_2 + 2H_2O \leftrightarrow NH_3\cdot(CH_2)_2\cdot NH_3 + 2OH^-. \quad (3)$$

Thus, $Zn(OH)_2$ and ZnO will be formed under the hydrothermal condition by

$$Zn^{2+} + 2OH^- \rightarrow Zn(OH)_2 \rightarrow ZnO + H_2O. \quad (4)$$

Two types of organic molecules are present in the reaction system, i.e., $NH_3\cdot(CH_2)_2\cdot NH_3$ (abbr. as en–H2) and hydrolyzed HMT, and their combined effects on the nucleation and growth process of ZnO are expected to promote the development of FZNs.

Fig. 1 illustrates X-ray diffraction pattern of as-deposited FZNs on Si substrate. Two obvious diffraction peaks were recorded on the spectrum, which can be well indexed to (100) and (101) planes of ZnO with hexagonal wurtzite structure (JCPDS No. 36-1451). No diffraction along (002) plane was detected, which may be related to the fact that most ZnO pedals are grown parallel to the substrate and that their growth directions are along (002) plane (as will be seen in the following content). In addition, no diffraction peak of other minerals such as $Zn(OH)_2$ was detected, indicating the obtained sample possesses high phase purity.

Fig. 2 illustrates SEM micrographs of FZNs on Si substrate. The low-resolution image (Fig. 2(a)) shows that, all ZnO flowers are in the size of 1–3 μm, and the distribution of ZnO flowers on the substrate is fairly uniform. The magnified SEM images in Fig. 2(b)–(d) clearly reveal that obtained ZnO exhibits the well-defined flowerlike morphology in their geometrical features. Three types of flowerlike morphology can be identified, i.e., flower cluster formed by accumulation of different flowers (Fig. 2(b)), isolated flower with multilayer pedals (Fig. 2(c)), and isolated flower with

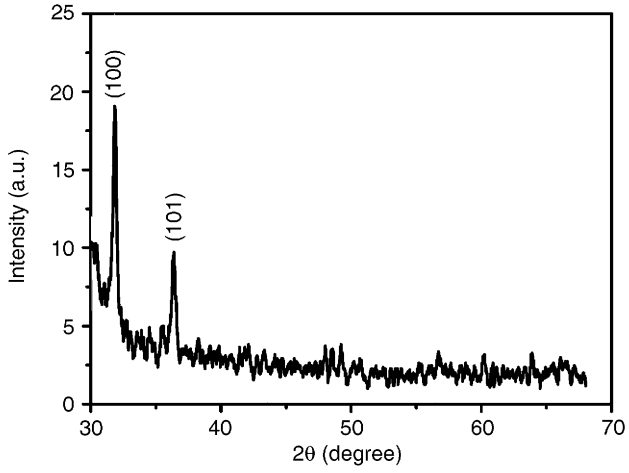

Fig. 1. XRD patterns of FZNs deposited on Si substrate.

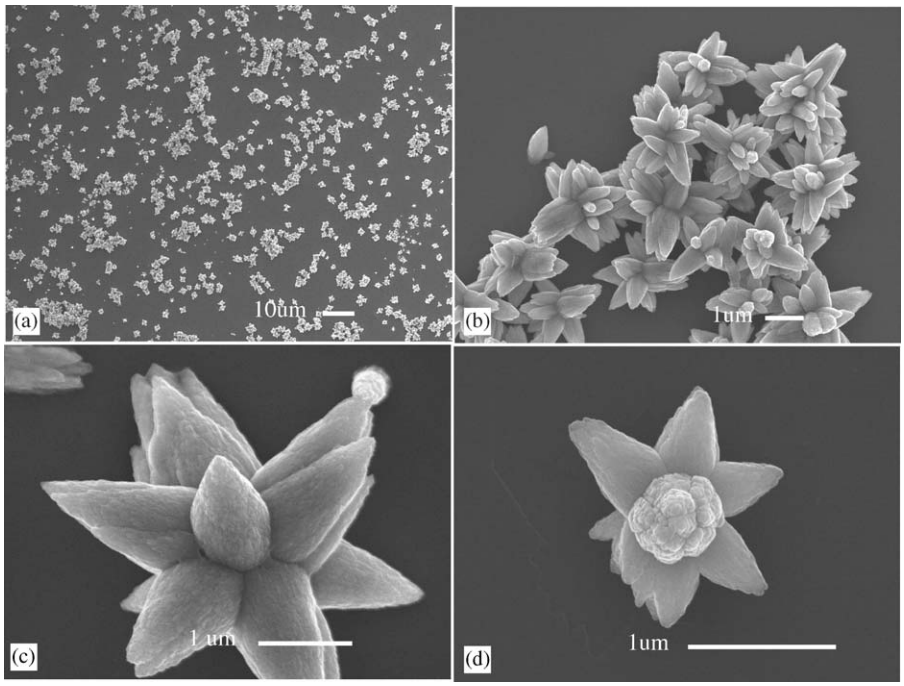

Fig. 2. SEM micrographs of flowerlike ZnO structures. (a) Low-resolution image, (b) ZnO flower cluster, (c) isolated ZnO flower with multilayer pedals, and (d) isolated ZnO flower with monolayer pedals.

monolayer pedals (Fig. 2(d)). Both types of isolated flower possess similar configuration, i.e., an upstanding style crystal and some flatly lying pedal crystals surrounding the style crystal. In contrast, for the flower cluster, usually no style crystal can be distinguished. Moreover, all the flower pedals exhibit the tapering feature with the root size of 300–500 nm and the tip size of 30–50 nm in average, which is different from FZNs consisting of swordlike ZnO nanorods by the cetyltrimethylammonium bromide-assisted hydrothermal process [14].

Fig. 3(a)–(d) illustrates the representative TEM micrographs of two typical ZnO flowers in the same sample and corresponding selective area electron diffraction (SAED) patterns. Fig. 3(a) gives the structure of a typical ZnO flower with better crystallinity and SAED pattern of individual pedal crystal (inset). The tip structure of the pedal shows that it is not a single crystal rod, but an assembly of several well-aligned nanorods. The SAED pattern indicates the single crystal nature of a single nanorod and the growth direction along (0002) plane. Fig. 3(b) gives the structure of a ZnO flower with well-arranged pedals and less crystallization. The magnified tip structure of the individual pedal shown in Fig. 3(c) illustrates that the pedal is also built up by many well-aligned nanorods but with smaller diameter (~5 nm), which possesses considerable similarity to the pedal structure in Fig. 3(a). Correspondingly, the SAED pattern presented in the inset of Fig. 3(c) is characterized by the symmetrical stripes rather than polycrystalline circles or arrayed spots, justifying the presence of some ordered arrangement of crystallites in the pedal. Fig. 3(d) presents the structure of the style crystal, which is located at the center of pedals and is probably grown parallel to the incidence direction of the electron beam. Results show that the style crystal is built up by several closely packed particles, and the strong and well-arrayed spots in the inset SAED pattern indicate the single crystalline nature of individual component particle and the crystal growth along (0002) plane. The fact that two different flowerlike structures with similar features occur in one sample indicates that the deposition of FZNs may be a time-dependent process, and the FZNs formed at different period will exhibit different structure correspondingly. In view of the principle that the hydrothermal process can promote the crystal growth, we suggest that the ZnO flower with better crystallinity may be formed earlier than that with less crystallinity.

The crystallographic morphology of ZnO can be influenced by many experimental parameters such as the basicity of the reaction system, precursor, solvent, time and temperature, etc. Among these parameters, the precursor composition is found to have determinative effects on the flowerlike morphology of ZnO in the investigated aqueous system. Therefore, we have presented preliminary results on the precursor-dependent morphology of ZnO in this paper. Morphologies of three control samples without en (sample 2), without HMT (sample 3), and with lower zinc–en ratio

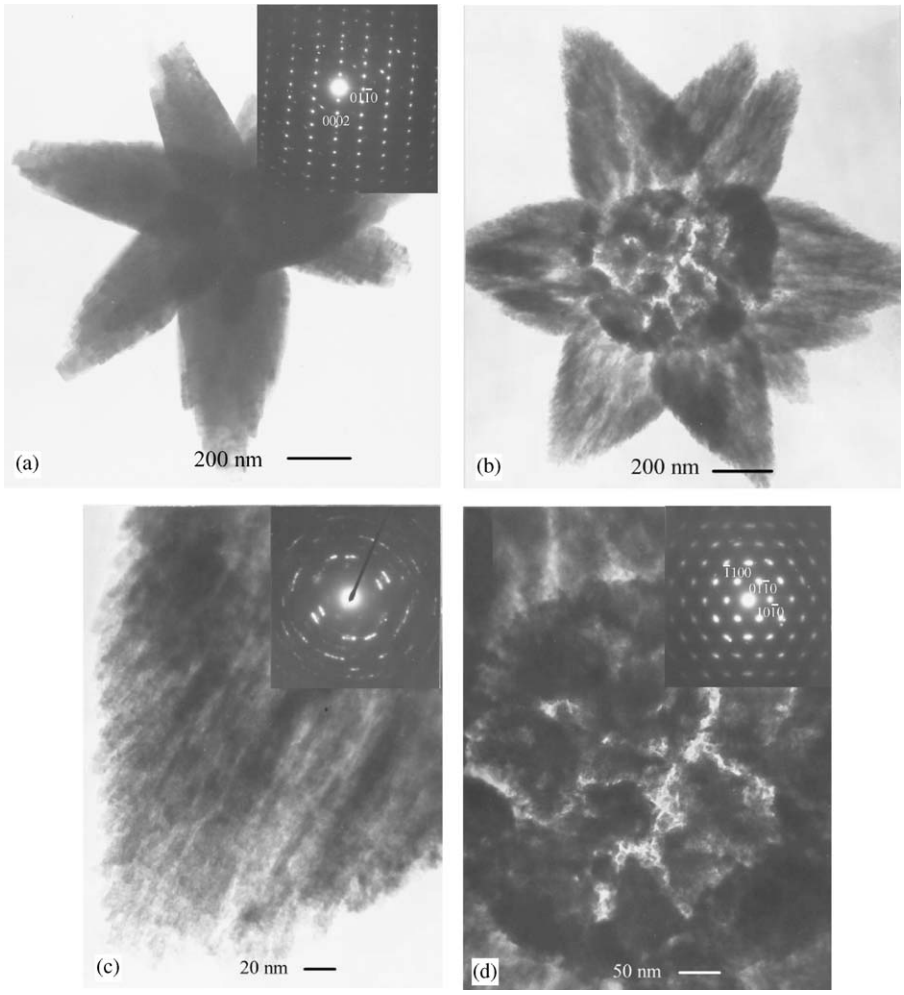

Fig. 3. TEM micrographs of flowerlike ZnO structures. (a) ZnO flower with better crystallinity, and SAED of one pedal tip (inset), (b) ZnO flower with less crystallinity, (c) the tip structure of one pedal in (b) and its SAED pattern (inset), and (d) the structure of style crystal in (b) and its SAED pattern (inset).

(1:6, sample 4) were compared with sample 1, with the intent to examine the function of en and HMT during the deposition process of FZNs. Fig. 4 illustrates SEM images of ZnO structure of samples 2–4.

Such following results can be obtained by comparing Figs. 2 and 4. When only HMT was used as the supplier of OH^-, $Zn(OH)_2$ nanosheet rather than flowerlike ZnO was obtained, as shown in Fig. 4(a). When only en was used, ZnO structures with flowerlike morphology can be obtained, but with the formation of many nanorods (~200–300 nm in diameter) on substrate, as shown in Fig. 4(b). These ZnO rods may originate from the heterogeneous deposition of ZnO on Si substrate at the initial stage of the thermolysis of zinc–en complex. When both HMT and en were used, most products are in the flowerlike morphology and very few nanorods were produced, as shown in Fig. 2. These results show that en has determinant effects on the formation of flowerlike structures on one hand, and HMT can modify the nucleation and growth process of ZnO crystal in the hydrothermal synthesis on the other. During the heating process up to 95 °C, HMT will hydrolyze and release OH^- into solution by Eq. (2), leading to the increase of both the concentration of OH^- and the ionic product of $Zn(OH)_2$. So the heterogeneous precipitation of $Zn(OH)_2$ on substrate, which requires lower ionic product than the homogeneous precipitation, can be effectively prevented in the initial stage of the thermolysis process.

The actual function of en in the formation process of FZNs can be obtained by analyzing the morphology of samples with different zinc–en ratios. The zinc–en ratio of 1:3 means that the amount of en is just enough to complex all the zinc ions in precursor and form a clear precursor solution. Correspondingly, clearly defined ZnO flowerlike structures were obtained, and almost all pedal crystals exhibit a tapering feature, as illustrated in Fig. 2. When en was excessive to Zn^{2+} and the zinc–en ratio was 1:6, only isolated ZnO rods and a few sparsely distributed irregular aggregations of ZnO rods

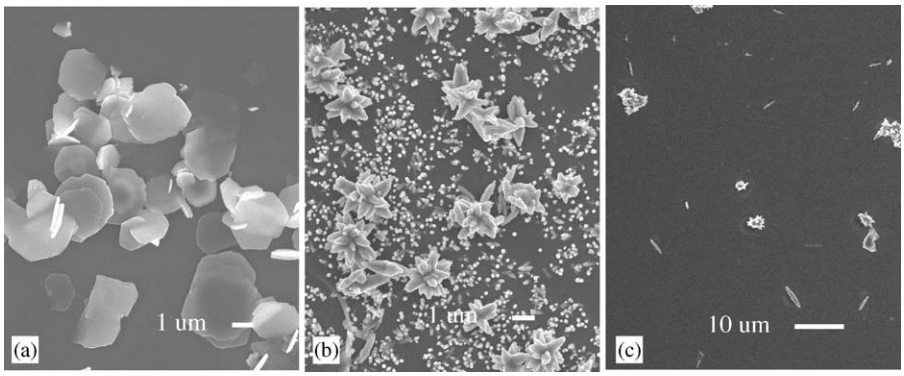

Fig. 4. SEM micrographs of ZnO structures with different precursors. (a) Zn–HMT ratio of 1:1 without en (sample 2), (b) Zn–en ratio of 1:2 without HMT (sample 3), and (c) Zn–HMT–en ratio of 1:1:6 (sample 4).

rather than FZNs were obtained (Fig. 4(c)). In addition, all ZnO rods in Fig. 4(c) exhibit smaller diameter, higher aspect ratio, and much less tapering feature. These results indicate that the proper zinc–en ratio is a key factor for the formation of tapering pedals of FZNs.

ZnO crystal is a polar crystal whose positive polar plane is rich in Zn and the negative polar plane is rich in O. When there is no organic additive in solution, spherical ZnO particles will be easily developed because of the Ostwald ripening process [21]. When en is present in the aqueous solution, en will hydrolyze and form en–H2 according to Eq. (3), which bears two positive charges. Thus by the coulomb interaction, en–H2 molecules will adsorb on the negative polar planes, retarding the growth rate of these planes. When the concentration of en is high enough, en–H2 molecules will cover all the side surface of ZnO crystal, thus enhancing the growth along (0002) plane greatly and resulting in the formation of rods with uniform diameter and high aspect ratio. When the concentration of en is relatively low, en–H2 molecules will be not enough to cover all the side surface of ZnO crystal. So both the impeding effect of en on the crystal growth and the Ostwald ripening process will take effect, resulting in the formation of pedal crystals with the obvious tapering feature. However, the exact formation mechanism of FZNs, i.e., how these tapering pedals assemble together and form ZnO flowers, is still not clear at the present stage. Further investigations on the time-dependent hydrothermal process are required.

Fig. 5 illustrates the photoluminescence spectrum of flowerlike ZnO structure under the photon excitation of 340 nm. A strong and sharp ultraviolet (UV) emission at 389 nm dominates the photoluminescence spectrum, with several weak emission peaks in blue and blue-green band (449, 467, 481, 493 nm). The FWMH of UV peak exhibits FWHM of about 5.4 nm, which is much smaller than the value of ZnO single crystal nanorod [22], ZnO nanoneedle [6], and ZnO flowers [5]. We suggest that this particular UV emission behavior may

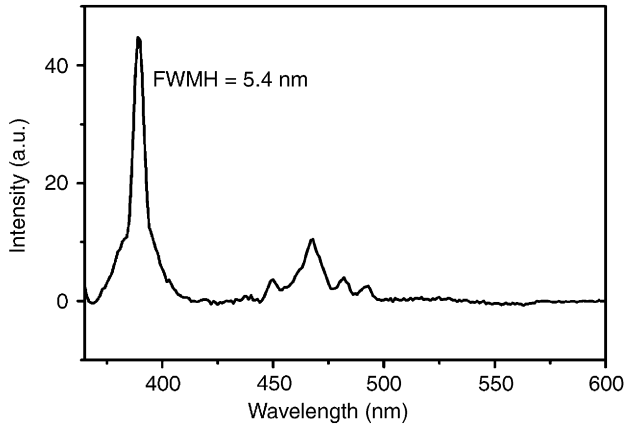

Fig. 5. Photoluminescence spectrum of flowerlike ZnO structures under the photon excitation of 340 nm at room temperature.

be mainly related to the special pedal structures in FZNs. As for the mechanism, it is commonly accepted that the UV emission should be attributed to the radiative annihilation of excitons [23,24], and the weak peaks in the blue-green band may originate from the electron transition from the level of the ionized oxygen vacancies to the valence band [25]. The sharp and intense UV emission, the weak emission related to ionized oxygen vacancies, and the absence of the well-known stronger and broader emission in the yellow-green band illustrate the good crystallization quality and the high stoichiometric nature of obtained products.

4. Conclusion

A novel and rapid solution route was proposed to fabricate ZnO nanostructures with well-defined flower-like morphology by the joint use of en and HMT. The flower pedals built up by many well-aligned nanorods are in the typical tapering feature with the tip size of 30–50 nm. The overall FZNs exhibit hexagonal wurtzite structure, strong UV emission, and uniform distribution

on substrate. Analysis shows that the capping reagent en and the zinc–en molar ratio have determinative effects on the formation of FZNs. In addition, HMT can meditate the nucleation and growth of ZnO crystal by modifying the solution basicity, thus inhabiting the formation of undesired nanorods on substrate. This work not only obtained FZNs, which possess great potential applications in various fields such as nanosensors and catalyst support, etc., but also afforded a simple and effective way to synthesis other similar oxides with complex morphology.

Acknowledgments

This work is financially supported by the Ministry of Science and Technology of China through 973-project under grant 2002CB613306.

References

[1] R.F. Service, Science 276 (1997) 895.
[2] Special issue on transparent conducting oxides, MRS Bulletin, August issue, 2000.
[3] S.C. Minne, S.R. Manalis, C.F. Quate, Appl. Phys. Lett. 67 (1995) 3918.
[4] M.H. Huang, S. Mao, H. Feick, H.Q. Yan, Y.Y. Wu, H. Kind, R. Russo, P.D. Yang, Science 292 (2001) 1897.
[5] J. Zhang, L. Sun, J. Yin, H. Su, C. Liao, C. Yan, Chem. Mater. 14 (2002) 4172.
[6] W.I. Park, G.C. Yi, M. Kim, S.J. Pennycook, Adv. Mater. 14 (2002) 1841.
[7] J.Q. Hu, Q. Li, X.M. Meng, C.S. Lee, S.T. Lee, Chem. Mater. 15 (2003) 305.
[8] J.Y. Lao, J.Y. Huang, D.Z. Wang, Z.F. Ren, D. Steeves, B. Kimball, W. Porter, Appl. Phys. A 78 (2004) 539.
[9] J.Y. Lao, J.Y. Huang, D.Z. Wang, Z.F. Ren, Nanoletters 3 (2003) 235.
[10] X.Y. Kong, Z.L. Wang, Nanoletters 3 (2003) 1625.
[11] X.Y. Kong, Y. Ding, R. Yang, Z.L. Wang, Science 303 (2004) 1348.
[12] J.Y. Lao, J.G. Wen, Z.F. Ren, Nanoletters 2 (2002) 1287.
[13] P.X. Gao, Z.L. Wang, J. Am. Chem. Soc. 125 (2003) 1299.
[14] H. Zhang, D. Yang, Y. Ji, X. Ma, J. Xu, D. Que, J. Phys. Chem. B. 108 (2004) 3955.
[15] Z. Wang, X.F. Qian, J. Yin, Z.K. Zhu, Langmuir 20 (2004) 3441.
[16] Z.R. Tian, J.A. Voigt, J. Liu, B. Mckenzie, M.J. Mcdermott, J. Am. Chem. Soc. 124 (2002) 12954.
[17] S. Lindroos, M. Leskela, Int. J. Inorg. Mater. 2 (2000) 197.
[18] D.S. Boyle, K. Govender, P. O'Brien, Thin Solid Films 431/432 (2003) 483.
[19] L. Vayssieres, Adv. Mater. 15 (2003) 464.
[20] D.S. Boyle, K. Govender, P. O'Brien, Chem. Commun. (2002) 80.
[21] J.A. Marqusee, J. Ross, J. Chem. Phys. 79 (1983) 373.
[22] L. Guo, Y.L. Ji, H. Xu, J. Am. Chem. Soc. 124 (2002) 14864.
[23] S. Monticone, R. Tufeu, A.V. Kanaev, J. Phys. Chem. B. 102 (1998) 2854.
[24] V.A. Dijken, E.A. Meulenkamp, D. Vanmaekelbergh, A. Meijerink, J. Lumin. 87–89 (2000) 454.
[25] D.H. Zhang, Q.P. Wang, Z.Y. Xue, Appl. Surf. Sci. 207 (2003) 20.